

Multi-Bunch Instabilities: Observations, Cures

Rolf-Dieter Kohaupt
 DESY, HAMBURG
 2000 Hamburg, 52

Abstract

In this article, observations and cures of instabilities are described. It is emphasized, that the most powerful cure of multi-bunch instabilities is an active damper system. The principle mechanism of a damper system is discussed and recent observations are presented.

1 INTRODUCTION

Multi-bunch instabilities can arise if electromagnetic fields having a decay time greater than the bunch spacing time are excited by single bunch motions within the components of the vacuum chamber. The forces then generated affect all bunches, so that they are all coupled. Therefore, the total beam current is the quantity that determines the growth rates and – together with the Landau damping – also the thresholds and the beam intensity limits. The strength of the electromagnetic fields can be described in terms of the impedances distributed around the vacuum chamber.

The single bunch motion is classified by internal modes. However, for sufficiently short bunches (proton bunches can be an exception) the dipole motion is most severe. Multi-bunch instabilities can become very strong in high energy electron machines. In these machines the impedance of the accelerating structure must be large, so that the level of the parasitic mode impedances is large as well. The parasitic modes then are the source of the strong multi-bunch instabilities limiting the beam currents far below design values. In order to demonstrate the methods of observation and cures the discussion is restricted to dipole oscillations excited by localized impedances especially in the case of electron machines.

2 REVIEW OF THE THEORY

The multi-bunch system can be described by a set of N differential equations, N being the bunch number (1):

$$\left(\frac{d^2}{dt^2} + \Omega^2\right) \mathbf{x}_\mu = \sum_{\nu=0}^{N-1} V_\mu(\mathbf{x}_0, \dots, \mathbf{x}_{N-1}) + F_\mu(\mathbf{x}_0, \dots, \mathbf{x}_{N-1}) + D_\mu(t); \mu = 0, \dots, N-1 \quad (1)$$

In this equation, t and ω are the time and the synchrotron frequency in the longitudinal, the quasi-time and the betatron frequency in the transverse direction. The forces in the ring are described by V , which is a linear functional of the dipole displacements \mathbf{x}_μ of the bunches. The forces F_μ are added to take care of an active damper system, which

will be discussed later. Finally $D_\mu(t)$ is an external force added in order to test the system by external excitation. Passing to the domain of complex frequencies ω eq. (1) becomes:

$$Q(w) \hat{\mathbf{x}}_\mu(w) = \sum_{\nu=0}^{N-1} \left(\hat{V}_{\mu\nu}(w) + \hat{F}_{\mu\nu}(w) \right) \hat{\mathbf{x}}_\nu + \hat{D}_\mu(w) \quad (2)$$

with

$$1/Q(w) = \sum_{l=-\infty}^{+\infty} \frac{1}{\Omega^2 - (l\omega_0 + w)^2} \quad (3)$$

ω_0 being the revolution frequency. The Fourier transforms $\hat{\mathbf{x}}_\mu(w)$ etc. are closely related to the z -transform of sampled data due to the fact that all exciting objects are localized. The equation (2) can be diagonalized in terms of the “normal mode” vectors:

$$\bar{K}_\tau = \frac{1}{\sqrt{N}} \left\{ \begin{array}{c} \vdots \\ e^{2\pi i \mu \tau / N} \quad e^{2\pi i \mu w / N \omega_0} \\ \vdots \end{array} \right\} \quad (4)$$

leading to the complex eigenfrequencies of the system, from (3) and (4), then one can derive:

$$V_{\mu\nu} = \sum_{\tau=0}^{N-1} \bar{K}_\tau(w) (iZ(\tau\omega_0 + w)) \bar{K}_\tau^*(-w^*) \quad (5)$$

$$F_{\nu\mu} = \sum_{\tau=0}^{N-1} \bar{K}_\tau(w) \tilde{F}(\tau\omega_0 + w) \bar{K}_\tau^*(-w^*) \quad (6)$$

where $Z(\tau\omega_0 + w)$ as the impedance functions and $\tilde{F}(\tau\omega_0 + w)$ is the transfer function of the damper system.

3 OBSERVATIONS AND CURES

If the beam oscillates according to a single normal mode r , one can observe a spectrum of frequencies.

$$\omega_r = lN\omega_0 \pm (\tau\omega_0 + \Delta\omega) \quad (7)$$

appearing as the upper (+ sign) and lower (-sign) sidebands of the bunch frequency lines $lN\omega_0$; $\Delta\omega$ denotes the synchrotron frequency in the longitudinal and the fractional betatron frequency in the transverse direction.

Fig. 1 shows the frequency interval between $lN\omega_0$ and $(l+1)lN\omega_0$

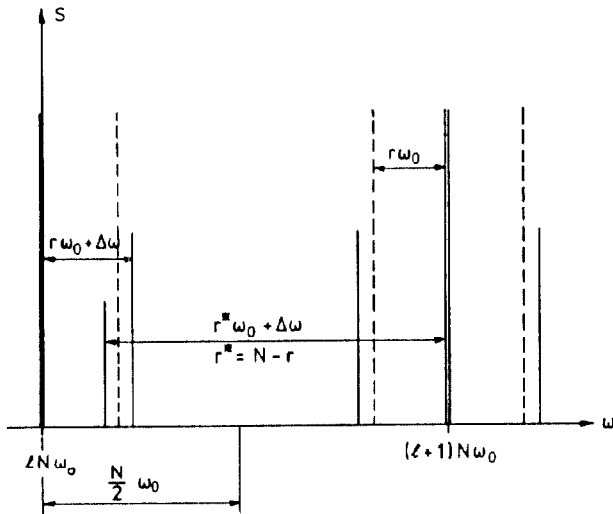


Figure 1. Normal Mode Spectrum

Let us consider r and $r^* = N - 1$, the “complementary” mode. According to fig. 1, the mode r produces the upper oscillation sideband and r^* produces the lower oscillation sideband around $lN\omega_0 + r\omega_0$. Instead of $r = 0, \dots, N - 1$ we consider the pairs $r \leq N/2, r^*$ (only for simplicity we assume N to be even). Then all modes can be observed in a frequency interval between $lN\omega_0$ and $lN\omega_0 + \frac{N}{2}\omega_0$ having a bandwidth of $\frac{N}{2}\omega_0$. From the theory of multi-bunch instabilities follows that any real part of the impedance Z around $lN\omega_0 + r\omega_0$ anti-damps the mode r and damps the mode r^* . That is true only in the longitudinal direction. In the transverse direction anti-damping and damping alternate. The stability properties of all the modes defined by all contributions of the impedance function from all the different bunch frequency intervals.

3.1 Observation of growth rates

In order to get information about the stability of all the modes it is possible to excite the beam on the different mode frequencies far below the threshold current, observing the damping rates as a function of beam current. Fig. 2 illustrates this method.

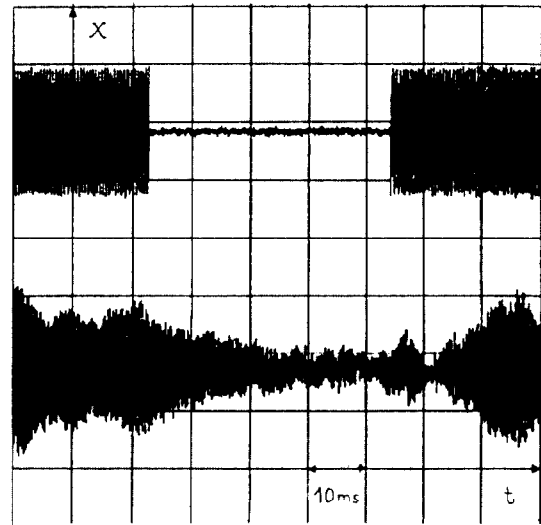


Figure 2. Response of an Excited Beam

The beam excitation on the mode frequency is “gated” as shown by the upper trace. The beam response is shown by the lower trace. After the excitation has been stopped the damping rate can be measured. The experiment was done at PETRA in the longitudinal direction. The damping time is about 15 m sec at low currents.

3.2 Reduction of impedances

If one has sufficient information about the dangerous parasitic modes a possible cure is to reduce the impedances of those modes by energy absorbing devices. This has been done in several machines. However, this method fails if the number of cavities and cells is too high (HERA-ring: about 100 cavities). Therefore, the only effective cure in all cases where a reduction of the impedances is not possible, is active damping by feedback systems.

3.3 Feedback systems

Due to the periodic structure shown in fig. 1, the effect of all impedance contributions can be represented by an equivalent effective impedance function restricted to a frequency interval with a bandwidth of half the bunch frequency. In order to keep the beam stable, we have to damp all the modes so that the damping rates exceed the growth rates. Therefore, we have to build up an “active impedance” function within a frequency range of $\frac{N}{2}\omega_0$. According to the stability properties between the modes, r and r^* the transfer function $\tilde{F}(r\omega_0 + \omega)$ has to obey the following relations.

$$1. \tilde{F}(r\omega_0 + \omega) \approx \tilde{F}(r\omega_0 + \omega) \text{ for } r \neq r^* \quad (8)$$

$$2. \text{Im } \tilde{F}(r\omega_0 + \omega) \text{ changes sign at } r\omega_0 \quad (9)$$

within a bandwidth $\frac{N}{2}\omega_0$. These properties can be represented by the following scheme:

$$\tilde{F}(\tau\omega_0 + \omega) = \tilde{F}_{NF}(\tau\omega_0 + \omega) \tilde{F}_c(\tau\omega_0 + \omega), \quad (10)$$

where $\tilde{F}_c(\tau\omega_0 + \omega)$ is sufficiently flat within $\frac{N}{2}\omega_0$ and $\tilde{F}_{NF}(\tau\omega_0 + \omega)$ is an "adjustable notch filter" described later.

3.4 Realization of feedback systems

The principal block diagram of a feedback system is shown in fig. 3

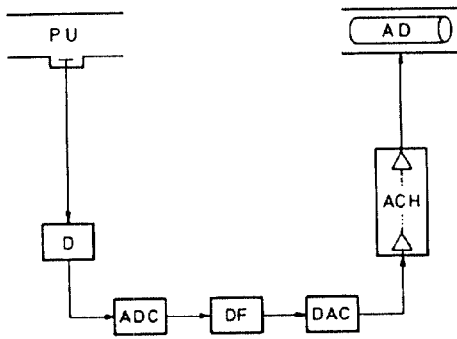


Figure 3. Block Diagram of a Feedback System

After the beam oscillations have been picked up (PU), the signals pass the detector (D). At the output the analog data will be converted to digital information (ADC). The "notch filter" properties of the transfer function are prepared by the digital filter unit (DF). Going back to analog data (DAC), the signals are transferred to a chain of amplifiers (ACH). At the end of the chain a power amplifier drives the active device (AD) which influences the beam. An example for an "adjustable notch filter" is given by

$$\tilde{F}_{NF} = e^{i\omega T} \left\{ \cos\varphi + \frac{4}{\pi} i \sin\omega T \sin\varphi \right\} \quad (11)$$

where φ can be adjusted such that the total transfer function \tilde{F} behaves like (8) and (9) for optimum damping. The transfer function (11) can be realized by a digital FIR-filter

$$G(\nu T_B) = \sum_{l=0}^2 T_l \cdot x(\nu T_B - lT) \quad (12)$$

In this relation x and g are input and output data respectively, T_B denotes the sampling time which is identical with the bunch spacing tune and T is the revolution time. Finally, the T_l represent the filter coefficients. In order to realize (11), one finds

$$T_0 = \frac{2}{\pi} \sin\varphi, T_1 = \cos\varphi, T_2 = -\frac{2}{\pi} \sin\varphi \quad (13)$$

3.5 Observations at high beam currents

For the PETRA and HERA electron rings transverse and longitudinal feedback systems have been built (2). The threshold currents in these machines are observed to be around 2.5 mA, whereas the designed currents are 60 mA. Therefore, the damping rates have to be improved by more than a factor 20. For PETRA the high current multi-bunch experiments have already been performed and a stable current of 56 mA has been reached in 80 bunches with a bunch frequency of 10 MHz. Fig. 4 shows the strong damping of the same mode shown in fig. 2 when the feedback loop is active.

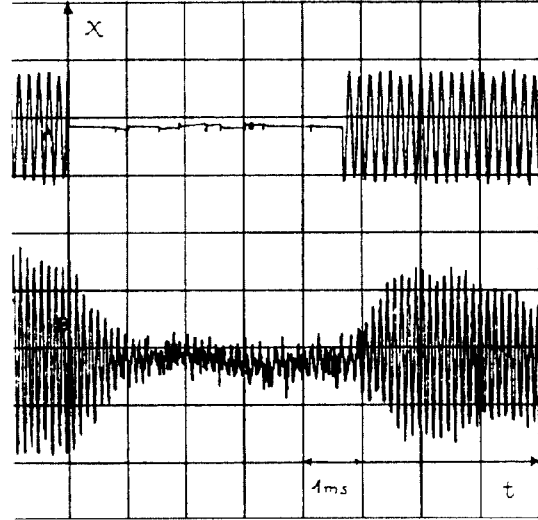


Figure 4. Damping of a Normal Mode by Feedback

3.6 Strong stability

As for as damping rates and growth rates are concerned, one would naively conclude that the relation

$$\delta_D > \delta_g \quad (14)$$

, where δ_D and δ_g are damping and growth rates respectively leads to a stable beam. However, even when the beam is "stable" there is still a strong coupling between the bunches. As a consequence, there is an energy transfer between the bunches. If a single bunch is excited, its energy is coupled to all the other bunches during the whole system is damped. If nearly all the bunches are excited with a tolerable amplitude, the energy can be transferred to a small number of bunches, so that their oscillation amplitude exceeds the tolerable limit. This internal "impact" is based on the real frequency shifts which are in general different for all modes and which are not compensated by the damper system. This "overshoot" effect increases if the number of bunches increases. The remaining damping rate at high currents has to be sufficiently large in order to keep the overshoot effect small. Since the real frequency shifts are of the same order as the growth rates (roughly) and since these shifts can be positive and negative, we

demand:

$$\delta_D - \delta_g \succ 2\delta_g \quad (15)$$

so that we obtain

$$\delta_D \succ 3\delta_g \quad (16)$$

instead of (14). The overshoot phenomena are still under theoretical investigation. For PETRA and HERA the feedback systems satisfy (16).

3.7 Observation of "overshoot" phenomena

The overshoot phenomena also influence the transfer of noise (always produced in a feedback loop) to the beam. This offers a method to observe overshoot effects by looking to the noisy motion of the beam. Therefore at PETRA we started with (16) at high currents and reduced the damping. But even at $\delta_D = 1.5\delta_g$ there was no significant increase of the noisy beam motion. However, the relation (16) should be satisfied in order to be save in the case of a high number of bunches (For the HERA-e ring $N = 220$).

4 REFERENCES

1. R.D. Kohaupt, DESY 91-071
2. M. Ebert et al. DESY 91-036